Monthly Notices of the ROYAL ASTRONOMICAL SOCIETY

MNRAS **499,** L26–L30 (2020) doi:10.1093/mnrasl/slaa150
Advance Access publication 2020 August 27

CO observations towards HI-rich Ultradiffuse Galaxies

Junzhi Wang,[1,2]★ Kai Yang,[2,3] Zhi-Yu Zhang,[4] Min Fang,[5] Yong Shi ,[4] Shu Liu,[6] Juan Li [1,2] and Fei Li[1,2]

[1]*Shanghai Astronomical Observatory, Chinese Academy of Sciences, 80 Nandan Road, Shanghai, 200030, China*
[2]*Key Laboratory of Radio Astronomy, Chinese Academy of Sciences, Nanjing, 210008, China*
[3]*I. Physikalisches Institut, Universität zu Köln, Zülpicher Str 77, D-50937 Köln, Germany*
[4]*School of Astronomy and Space Science, Nanjing University, Nanjing, 210093, China*
[5]*Department of Astronomy, California Institute of Technology, Pasadena, CA 91125, United States*
[6]*CAS Key Laboratory of FAST, National Astronomical Observatories, Chinese Academy of Sciences, Beijing 100012, China*

Accepted 2020 August 21. Received 2020 August 20; in original form 2020 May 29

ABSTRACT

We present CO observations towards a sample of six HI-rich Ultradiffuse galaxies (UDGs) as well as one UDG (VLSB-A) in the Virgo Cluster with the Institut de RadioAstronomie Millimétrique (IRAM) 30-m telescope. CO $J = 1$–0 is marginally detected at 4σ level in AGC 122966, as the first detection of CO emission in UDGs. We estimate upper limits of molecular mass in other galaxies from the non-detection of CO lines. These upper limits and the marginal CO detection in AGC 122966 indicate low mass ratios between molecular and atomic gas masses. With the star formation efficiency derived from the molecular gas, we suggest that the inefficiency of star formation in such HI-rich UDGs is likely caused by the low efficiency in converting molecules from atomic gas, instead of low efficiency in forming stars from molecular gas.

Key words: galaxies: ISM – galaxies: star formation.

1 INTRODUCTION

Ultradiffuse galaxies (UDGs) are extremely low-surface-brightness galaxies (LSBGs) at the optical and near-IR wavelengths (Papastergis, Adams & Romanowsky 2017). They have drawn much attention from both observers and theorists since the discovery of 47 UDGs in the Coma cluster (van Dokkum et al. 2015). Observations of UDGs mainly focused on optical and near-IR studies (van Dokkum et al. 2015; van der Burg, Muzzin & Hoekstra 2016; Yagi et al. 2016), which show that the stellar components are much less than those in normal galaxies. A subset of UDGs, which have high H I to stellar mass ratio and were normally found outside galaxy clusters, have been discovered in H I observations with large single-dish radio telescopes, such as Arecibo, Effelsberg and Green Bank Telescope (Roberts et al. 2004; Leisman et al. 2017; Spekkens & Karunakaran 2018). High angular resolution observations with radio interferometers (Leisman et al. 2017; Ball et al. 2018; Mihos et al. 2018; Brunker et al. 2019) showed that H I emission are more extended than the stellar components traced by optical images. The line widths (full width at half-maximum) of H I detected by single dishes (Roberts et al. 2004; Leisman et al. 2017; Spekkens & Karunakaran 2018) and interferometers (Leisman et al. 2017; Ball et al. 2018; Mihos et al. 2018) in such galaxies are only about or even less than 100 km s^{-1}. Such small linewidths led difficulties for determining dynamical mass of whole galaxy with large uncertainty of inclination angle.

With extremely high ratios of gas to stellar mass and with low stellar mass (Leisman et al. 2017; Mihos et al. 2018), such HI-rich UDGs should have inefficient star formation, low star formation rate (SFR), and low star formation efficiency (SFE) across cosmic time. HI-rich UDGs with a size of the Milky Way may be 'failed' $L_\star$ galaxies or 'failed' smaller galaxies, depending on the estimated halo mass (Leisman et al. 2017).

There are two major steps to form stars from H I gas: atomic gas converts to molecular gas, and molecular gas form stars. So, molecular to atomic gas fraction is a key parameter to understand the inefficient star formation in such galaxies. However, the lack of molecular gas information of such galaxies prohibits further distinction about which step is more crucial for the inefficient star formation in the history. Therefore, CO observations towards a sample of HI-rich local UDGs would help answer such questions: The inefficient star formation in such UDGs is caused by difficulties of forming molecular gas from atomic gas, or failed star formation from molecular gas?

Although there have been several CO observations with few detections (O'Neil, Hofner & Schinnerer 2000; Matthews & Gao 2001; Matthews et al. 2005; Das, Boone & Viallefond 2010; Cao et al. 2017) towards HI-rich LSBGs, which have quite high gas to star mass ratios, there is still no report on CO observations towards UDGs in the literature, up to now.

In this letter, we describe CO line observations and data reduction of a small sample of UDGs with the Institut de RadioAstronomie Millimétrique (IRAM) 30-m telescope in Section 2, present the main results and discussions in Section 3, and make the brief summary and future prospects in Section 4.

★ E-mail: jzwang@shao.ac.cn

2 OBSERVATIONS AND DATA REDUCTION

We select six HI-rich UDGs from the literature (Bellazzini et al. 2017; Leisman et al. 2017; Papastergis et al. 2017; Trujillo et al. 2017; Brunker et al. 2019) to perform CO line observations, because they have enough gas materials to form stars. The sample includes three Milky Way-sized ones with H I mass $\geq 10^9 M_\odot$, three dwarf galaxies with H I mass $< 2.5 \times 10^8 M_\odot$ (see Table 1), and VLSB-A, which is one of the three UDGs in the Virgo Cluster with velocity measured through optical spectra towards the nucleus (Mihos et al. 2015).

The observations were carried out from 2018 July 31 to August 3 with the IRAM 30-m millimetre telescope at Pico Veleta, Spain.[1] The Eight MIxer Receiver (EMIR) with dual polarizations, Fourier Transform Spectrograph (FTS) backend, and standard wobbler switching mode with ±120 arcsec offset at 0.5 Hz beam throw, were used. Focus calibrations were done at the beginning of the observations and during sunset or sunrise, towards planets or strong millimetre quasars. Pointing calibrations were done every 2 h using nearby quasars. CO(1–0) at E0 band and CO(2–1) at E2 band were covered simultaneously in our observations. The observing frequency of CO(1–0) varies from ∼112.35 GHz with typical system temperature of 150 K in SECCO-dI-1 to ∼115.273 GHz with typical system temperature of 300 K in VLSB-A. The system temperature also varies with different weather conditions and elevations of telescope. On the other hand, CO(2–1) observations are from ∼224.7 to 230.5 GHz, while the typical system temperature is about 500 K and strongly depends on weather conditions and elevations of telescope.

The pointing centre of each source is listed in Table 1. The optical images of these sources from the Palomar Transient Factory (PTF; Law et al. 2009; Rau et al. 2009) or the Zwicky Transient Facility (ZTF; Bellm et al. 2019) are presented in Figs 1 and 2.

The data were dumped every 1.7 min as one scan, and calibration was done every 6 scans. The beam sizes of the IRAM 30-m telescope are about 22 arcsec for CO(1–0) and 11 arcsec for CO(2–1), respectively. The conversion from T_A^* to T_{mb} is: $T_{mb} = T_A^* F_{eff}/B_{eff}$, where $F_{eff} = 95$ per cent and $B_{eff} = 81$ per cent for CO(1–0), while $F_{eff} = 92$ per cent and $B_{eff} = 59$ per cent for CO(2–1).

The CLASS package of GILDAS[2] was used for data reduction. The effective on-source time and the noise level for each source are listed in Table 2. First order baseline fitting was done for each spectrum with 1.7 min integration time. Then we smoothed and resampled each spectrum to ∼10 km s^{-1}, before averaging all spectra of each target (Fig. 1) with a weighting of $1/T_{sys}^2$. For each target, we calculated the standard deviation of each channel across all spectra. This gives a channel-based noise, which is pretty flat for all sources and is consistent with the *rms* value from the final spectrum obtained with standard method using class task 'average' f in each source. Even though the rms noise increases with the increasing of the frequency at 3 mm band due to the O_2 line in the Earth's atmosphere, it is almost the same within ±500 km s^{-1} for the observed CO(1–0) line.

The noise level (σ) in T_{mb} for each source is listed in Table 2, and are obtained from the averaged spectrum at the original frequency resolution (0.195 MHz), with line free channels using CLASS task 'base' with first-order polynomial. The upper limits of flux are calculated with $3\sigma \times \sqrt{\delta v \times \Delta V}$, where σ is the rms noise from the final spectrum for each source with 0.195 MHz resolution, δv is the velocity resolution corresponding to 0.195 MHz (∼0.5 km s^{-1}), and ΔV is 50 km s^{-1}, as the assumed line width. For most of the sources, since the observations were done in summer time, CO(1–0) data were much better than CO(2–1) due to weather conditions. Thus, CO(1–0), instead of CO(2–1) data, are used for estimation of the upper limits.

[1]Based on observations carried out with the IRAM 30-m telescope. IRAM is supported by INSU/CNRS (France), MPG (Germany), and IGN (Spain).
[2]http://www.iram.fr/IRAMFR/GILDAS

3 RESULTS AND DISCUSSION

CO(1–0) emission is marginally detected in AGC 122966 at 4σ level with velocity integrated flux of 0.23 ± 0.057 K km s^{-1} in T_{mb} (see Fig. 1), while only upper limits can be estimated in other sources. The velocity range of CO(1–0) emission in AGC 122966 is from about +50 to +150 km s^{-1}, relative to the systematic velocity obtained from the H I 21-cm emission.

The CO(2–1) line of AGC 122966, which was obtained simultaneously, was not detected at 3σ. The non-detection of CO(2–1) may be caused by the high system temperature at the 1.3 mm band. Furthermore, CO(2–1) has smaller beam size, which is only 25 per cent of the CO(1–0) beam coverage. So, if the CO emission is clumpy and located off the pointing centre of this observation, it is possible that CO clump is not fully covered by the CO(2–1) beam. To present the difference of the beam sizes, we overlay the beams on the stacked *R*-band images of AGC 122966, which are from the intermediate PTF survey, and show it in Fig. 1.

The velocity integrated luminosity of CO(1–0) (L_{CO}) in AGC 122966 is 2.2 ± 0.54 K km s^{-1} pc^{-2}, using the formula $\frac{\pi}{4\ln 2}\theta_{mb}^2 I \times D_L^2 \times (1+z)^{-3}$ (Solomon et al. 1997; Gao & Solomon 2004; Jiang et al. 2015), where $\theta_{mb} = 22$ arcsec is the main beam size of the observation, I is the velocity integrated flux in T_{mb}, D_L is the luminosity distance of the galaxy, and z is the redshift. The CO(1–0) emission is out of H I velocity range (Leisman et al. 2017; Mancera Piña et al. 2019) within ±45 km s^{-1}. The marginal detection of CO(1–0) might not be real because of the different velocity ranges of H I and CO(1–0). However, even though no related H I 21-cm line emission at the same velocity range as that of the CO(1–0) peak are reported, weak H I 21 cm below the detection limit in the literature are still possible, which means that the CO(1–0) detection can still be real. Last, even if the 3σ upper limit of CO(1–0) is adopted to estimate molecular gas mass of AGC 122966, instead of using the detection, the main result is still similar to considering this feature as detection.

The metallicity in UDGs is difficult to be measured due to weak optical emission. Only SECCO-dI-2 and UGC 2162 have such measurements in the literature, which gave low metallicities of 8.2 ± 0.2 of 12+log(O/H) for SECCO-dI-2 (Bellazzini et al. 2017) and 8.22 ± 0.07 of 12+log(O/H) for UGC 2162 (Trujillo et al. 2017), respectively. SECCO-dI-2 and UGC 2162 do not follow the mass–metallicity relation in galaxies (Berg et al. 2012), which gave the metallicity of ∼7.6 for 12+log(O/H) for galaxies with similar mass to SECCO-dI-2 as $M_* = 0.9 \times 10^7 M_\odot$ (Bellazzini et al. 2017) or UGC 2162 as $M_* = 2.0 \times 10^7 M_\odot$ (Trujillo et al. 2017). A tentative evidence that the gas-phase metallicities in diffuse systems are high for their stellar mass had been found in two UDGs (Greco et al. 2018). With limited information of metallicity measurement towards these UDGs, we would like to assume similar metallicity to that of SECCO-dI-2 in these UDGs in our discussion.

For galaxies with a metallicity of 8.2 ± 0.2, the conversion factor (α_{CO}), which converts from CO luminosity to molecular mass, should be higher than that in the Milky Way, based on the relation of metallicity and α_{CO} (Bolatto, Wolfire & Leroy 2013; Shi et al. 2016). α_{CO} (8.6 $M_\odot$/K km s^{-1}pc^2), with twice of that in the Milly Way

Table 1. Source list.

Source name	RA(J2000)	DEC(J2000)	cz km s^{-1}	Distance Mpc	r_e kpc	M_{HI} 10^9 M$_\odot$	M_{HI}/M_*	SFR M$_\odot$ yr^{-1}	References
AGC 122966	02:09:29.0	+31:51:15.0	6518	90	7.4 ± 3.3	1.0	8.3	0.022	1
SECCO-dI-1	11:55:58.5	+00:02:36.3	7791	112	2.6	1.2	120	–	2
AGC 334315	23:20:11.0	+22:24:10.0	5100	73	4.2 ± 1.1	1.4	23	0.045	1
UGC 2162	02:40:23.1	+01:13:45.0	1172	12.3	1.7	0.19	10	8.7×10^{-3}	3
SECCO-dI-2	11:44:33.8	−00:52:00.9	2543	40	1.3	0.24	27	–	4
Coma P	12:32:10.3	+20:25:23.0	1348	5.5	<1	0.035	81	3.1×10^{-4}	5
VLSB-A	12:28:15.9	+12:52:13.0	−120	16.5	9.7	–	–	–	6

Notes. The sources are separated into three sub-groups: Milky Way size HI-rich UDGs (AGC 122966, SECCO-dI-1, and AGC 334315), dwarf HI-rich UDGs (UGC 2162, SECCO-dI-2, and Coma P), and one UDG without H I detection in the Virgo Cluster.
References:1. Leisman et al. (2017), 2. Bellazzini et al. (2017), 3. Trujillo et al. (2017), 4. Papastergis et al. (2017), 5. Brunker et al. (2019), 6. Mihos et al. (2015)

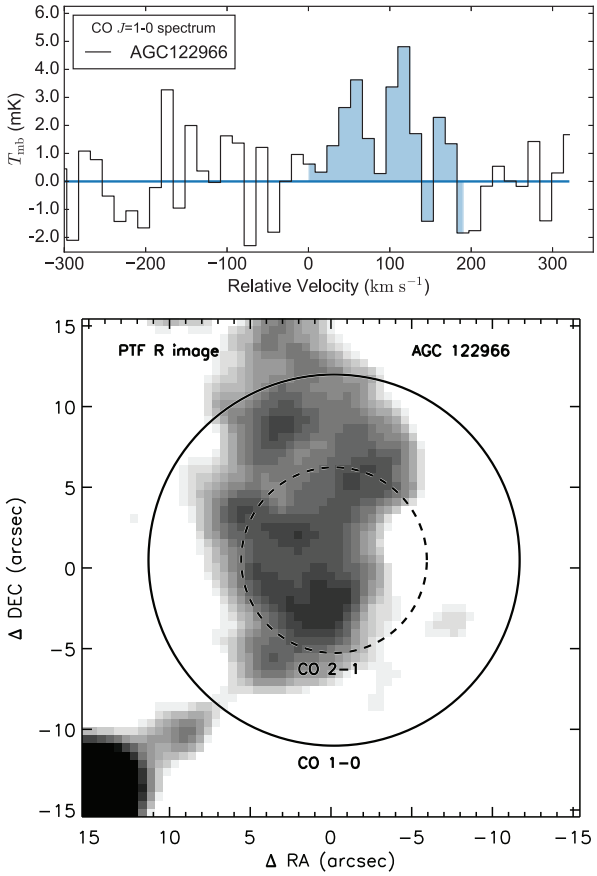

Figure 1. Top panel: CO(1–0) spectrum of AGC 122966 obtained with IRAM 30-m telescope, with velocity resolution of 14.53 km s^{-1}. Bottom panel: The beams of IRAM 30-m telescope for CO(1–0) (solid circle) and CO(2–1) (dashed circle) overlaid on the PTF (Law et al. 2009; Rau et al. 2009) *R* band of AGC 122966.

as a reasonable value for such metallicity, is adopted (see Table 2). The molecular gas mass in AGC 122966 is then estimated to be $1.9 \pm 0.46 \times 10^8$ M$_\odot$, if the emission feature is real. The H_2/H I mass ratio is 0.19 ± 0.05, while it ranges from ∼0.03 to 3 in a large sample of galaxies (Jiang et al. 2015).

Using the same method as for AGC 122966, the non-detection of CO emission in most of these HI-rich UDGs can give 3σ upper limits of molecular gas mass, assuming a line width of 50 km s^{-1} in each galaxy. Upper limits of H_2/H I mass ratios for each galaxy can also be estimated (see Table 2), which are from 0.012 in UGC 2162 to 0.083 in SECCO-dI-1. The upper limit of molecular gas mass is also estimated for AGC 122966 if that emission feature is not real. The 3 σ upper limit of CO(1–0) in AGC 122966 is about 1/4 of the flux of that feature, not only because that feature is only 4σ, but also because the line width of that feature is more than 50 km s^{-1}. Note that the pointing centres of our observations are with about 15 arcsec and 9 arcsec offsets from the optical centres in AGC 334315 and CO Mapping Array Pathfinder (ComaP; see Fig. 2.), respectively. The offset for AGC 334315 is about 70 per cent beam size of CO(1–0), while it is about 40 per cent for ComaP. Most of the emission at optical band in ComaP can be covered with the beam of CO(1–0) observation. However, only 1/3 to 1/2 of the optical emission region in AGC 334315 can be covered by CO(1–0) beam. Such offset can cause underestimation of CO upper limit in these two galaxies, which can further cause about a factor of 2 in ComaP or 3 in AGC 334315 underestimation of H_2/H I ratio and overestimation of SFR/M_{H_2}.

The ratio of molecular mass and stellar mass, M_{H_2}/M_*, in each galaxy, is also derived and listed in Table 2. The upper limits of this ratio range from 0.12 to 10, while this ratio ranges from ∼0.01 in massive galaxies with $M_* \sim 10^{11.5}$ M$_\odot$ to ∼1 in low mass end with $M_* \sim 10^{8.5}$ M$_\odot$, decreasing with M$_*$ at the massive end and flatten at the low mass end with large scatter (Jiang et al. 2015). No clear difference of M_{H_2}/M_* between HI-rich UDGs to normal galaxies can be justified with current results. On the other hand, the ratios of M_{HI}/M_* in these HI-rich UDGs, range from 8.3 to 120, are much higher than that in normal galaxies ranging from ∼0.01 at massive part to almost ten in the low mass end (Jiang et al. 2015).

The low H_2/H I mass ratios, i.e. the lack of molecular gas, in these HI-rich UDGs, all of which are less than 0.1 (see Table 2), might be the main reason of inefficient star formation, while such ratio in normal galaxies are from ∼0.03 to ∼3 with a median value of ∼0.3 (Jiang et al. 2015). If only the molecular gas was used for calculating SFE (SFR/M_{H_2}), such value will not be significantly lower than that in nearby spirals as $(5.25 \pm 2.5) \times 10^{-10}$ yr^{-1} (Leroy et al. 2008). The SFR in AGC 122966, the one with tentative CO(1–0) detection, is 0.022 M$_\odot$ yr^{-1} (Leisman et al. 2017), which gives an SFE of 1.3×10^{-10} yr^{-1}. On the other hand, with an SFR of 0.045 M$_\odot$ yr^{-1} (Leisman et al. 2017) and a non-detection of CO(1–0) in AGC 334315, the derived SFE with molecular gas is greater than 12.1×10^{-10} yr^{-1}, which is much higher than that in nearby spirals. Therefore, we suggest that the inefficient star formation

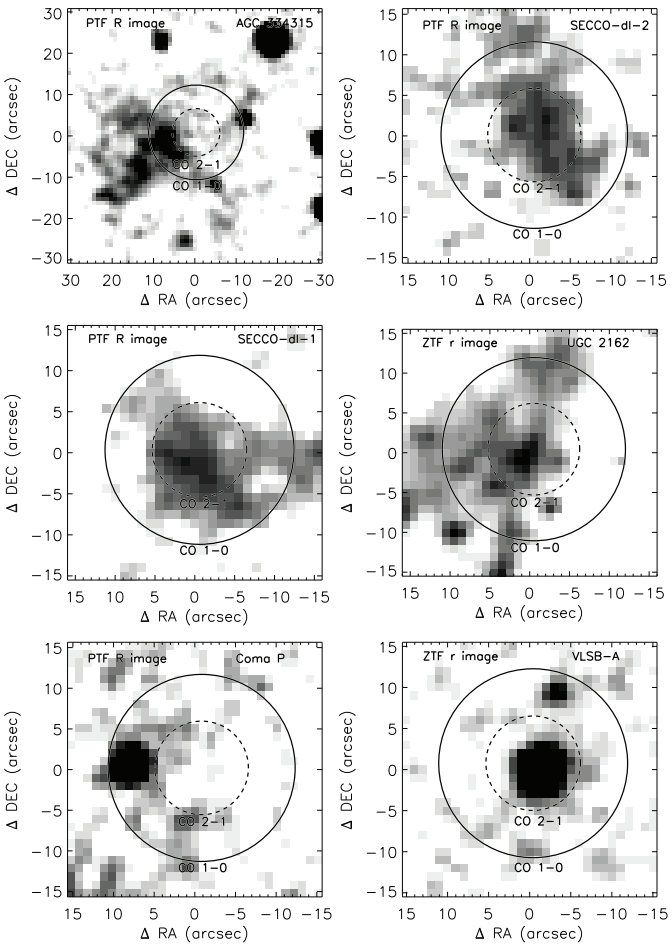

Figure 2. The beams of IRAM 30-m telescope for CO(1–0) (solid circle) and CO(2–1) (dashed circle) overlaid on the PTF (Law et al. 2009; Rau et al. 2009) *R* band or ZTF (Bellm et al. 2019) *r*-band images of individual UDGs.

Table 2. Observational results.

Source name	On-source time Minutes	rms[a] mK	I(CO 1-0)[b] K km s^{-1}	L(CO) 10^7 K km s^{-1} pc^{-2}	M_{H_2}[c] 10^8 M$_\odot$	M_{H_2}/M_{HI}	M_{H_2}/M_*	SFR/M_{H_2} 10^{-10} yr^{-1}
AGC 122966	336	3.5	0.23 ± 0.057	2.2 ± 0.54	1.9 ± 0.46	0.19 ± 0.05	1.6 ± 0.4	1.3
	–	–	<0.053[d]	<0.50	<0.43	<0.043	<0.36	>5.7
SECCO-dI-1	316	5.2	<0.078	<1.2	<1.0	<0.083	<10.0	–
AGC 334315[e]	432	4.4	<0.066	<0.43	<0.37	<0.026	<0.60	>12.1
UGC2162	107	9.6	<0.14	<0.027	<0.023	<0.012	<0.12	>37.8
SECCO-dI-2	294	5.7	<0.086	<0.17	<0.15	<0.071	<1.9	–
Coma P[e]	95	19.6	<0.29	<0.011	<0.0095	<0.027	<2.2	>3.3
VLSB-A	121	12.5	<0.19	<0.067	<0.058	–	–	–

[a] In $T_{\rm mb}$ with frequency resolution of 0.195 MHz, which corresponds to ~ 0.5 km s^{-1} at 115 GHz.
[b] 3σ upper limits for velocity integrated flux for 50 km s^{-1} line width in $T_{\rm mb}$.
[c] αCO $= 8.6$ M$\odot$/K km s^{-1} pc^2 is used for estimating molecular gas mass.
[d] 3σ upper limit estimation for AGC 122966 if that feature is not real.
[e] The offsets of the pointing centres to the centres of optical emission is about 15 arcsec for AGC 334315 and 9 arcsec for Coma P, which can cause underestimation of the upper limits of CO emission in these two galaxies.

in such galaxies is mainly due to the low efficiency of forming molecules from atomic gas, instead of forming stars from molecular clouds.

With limited information of metallicity in these UDGs, the adopted α_{CO} may be lower than the real value, which would underestimate molecular gas mass. In this case, low SFE for molecular gas cannot be the only explanation of inefficient star formation in such HI-rich UDGs. Deep CO observations towards UDGs with Atacama Large Millimeter-Submillimeter Array (ALMA), as well as metallicity measurement with deep optical spectroscopic observations, will

help us to derive molecular gas mass and determine the reason of inefficient star formation.

Since molecular gas and stellar masses are much less than the atomic mass in such galaxies, the baryonic mass can be estimated with only H I, to derive the dynamical-to-baryonic mass ratios. As discussed in the literature (Leisman et al. 2017; Brunker et al. 2019), the total masses estimated with dynamics are not massive enough, such HI-rich UDGs should not be failed $L_\star$ spiral galaxies, even though some of them have H I and optical sizes similar to those of $L_\star$ spiral galaxies.

The properties of such galaxies, such as high halo spin parameters (Leisman et al. 2017), may bring down the efficiency of forming molecules from atomic gas. AGC 122966, with marginal detection of CO(1–0) emission, is the galaxy with lowest M_{HI}/M_* ratio (see Table 1) among the 6 HI-rich UDGs. The relatively high H_2/H I ratio in AGC 122966 may cause higher SFR than other HI-rich UDGs in the past and nowadays, which can further explain the relatively low M_{HI}/M_* ratio in AGC 122966; or, if that emission feature is not real, AGC 122966 will be similar to other UDGs. Further confirmation of CO emission in AGC 122966 with millimetre interferometers, such as ALMA or Northern Extended Millimeter Array (NOEMA), is necessary to make a conclusion.

4 SUMMARY AND FUTURE PROSPECTS

As the first survey observations of CO(1–0) and CO(2–1) towards a sample of HI-rich UDGs with the IRAM 30-m telescope, we marginally detected CO(1–0) in one galaxy (AGC 122966) at 4σ level. The non-detection of CO lines in other sources provides good upper limits of molecular masses, which help estimate upper limits of molecular gas mass. We find low ratios of molecular to atomic mass, which indicate that the inefficient star formation in such HI-rich UDGs should mainly be caused by the difficulty of forming molecules from atomic gas, while the SFE derived for molecular gas is not significantly lower than normal spirals. An alternative possibility is that CO lines are no longer good tracers of molecular gas in UDGs, because the metallicity might be lower than assumed.

Further, large-sample high-sensitivity CO observations with ALMA can better derive molecular mass in such galaxies and can better provide the molecular to atomic mass ratios. ALMA observations can also provide the spatial distribution of molecular gas, which can be used to compare with star formation information using further optical emission line observations.

ACKNOWLEDGEMENTS

We thank the referee, Dr U. Lisenfeld, for helpful suggestions to improve the manuscript. This work is supported by National Key Basic Research and Development Program of China (grant no. 2017YFA0402704) and the National Natural Science Foundation of China grant 11590783 and U1731237. This study is based on observations carried out under project number 068-15 with the IRAM 30-m telescope. IRAM is supported by INSU/CNRS (France), MPG (Germany), and IGN (Spain). This work is also benefited from the International Space Science Institute (ISSI/ISSI-BJ) in Bern and Beijing, thanks to the funding of the team 'Chemical abundances in the ISM: the litmus test of stellar IMF variations in galaxies across cosmic time' (Principal Investigator DR and ZYZ). JW thanks Dr Yu Lu for helpful discussion about UDGs.

DATA AVAILABILITY

The original CO data observed with IRAM 30-m telescope can be accessed by IRAM archive system at https://www.iram-institute.org/EN/content-page-386-7-386-0-0-0.html, while optical images can be obtained from PTF and ZTF archive systems. If anyone is interested in the reduced data presented in this paper, please contact Junzhi Wang at jzwang@shao.ac.cn.

REFERENCES

Ball C. et al., 2018, AJ, 155, 65
Bellazzini M., Belokurov V., Magrini L., Fraternali F., Testa V., Beccari G., Marchetti A., Carini R., 2017, MNRAS, 467, 3751
Bellm E. C. et al., 2019, PASP, 131, 018002
Berg D. A. et al., 2012, ApJ, 754, 98
Bolatto A. D., Wolfire M., Leroy A. K., 2013, ARA&A, 51, 207
Brunker S. W. et al., 2019, AJ, 157, 76
Cao T. W. et al., 2017, AJ, 154, 116
Das M., Boone F., Viallefond F., 2010, A&A, 523, A63
Gao Y., Solomon P. M., 2004, ApJS, 152, 63
Greco J. P., Goulding A. D., Greene J. E., Strauss M. A., Huang S., Kim J. H., Komiyama Y., 2018, ApJ, 866, 112
Jiang X. J., Wang Z., Gu Q., Wang J., Zhang Z. Y., 2015, ApJ, 799, 92
Law N. M. et al., 2009, PASP, 121, 1395
Leisman L. et al., 2017, ApJ, 842, 133
Leroy A. K., Walter F., Brinks E., Bigiel F., de Blok W. J. G., Madore B., Thornley M. D., 2008, AJ, 136, 2782
Mancera Piña P. E. et al., 2019, ApJ, 883, L33
Matthews L. D., Gao Y., 2001, ApJ, 549, L191
Matthews L. D., Gao Y., Uson J. M., Combes F., 2005, AJ, 129, 1849
Mihos J. C. et al., 2015, ApJ, 809, L21
Mihos J. C., Carr C. T., Watkins A. E., Oosterloo T., Harding P., 2018, ApJ, 863, L7
O'Neil K., Hofner P., Schinnerer E., 2000, ApJ, 545, L99
Papastergis E., Adams E. A. K., Romanowsky A. J., 2017, A&A, 601, L10
Rau A. et al., 2009, PASP, 121, 1334
Roberts S. et al., 2004, MNRAS, 352, 478
Shi Y., Wang J., Zhang Z. Y., Gao Y., Hao C. N., Xia X. Y., Gu Q., 2016, Nat. Commun., 7, 13789
Solomon P. M., Downes D., Radford S. J. E., Barrett J. W., 1997, ApJ, 478, 144
Spekkens K., Karunakaran A., 2018, ApJ, 855, 28
Trujillo I., Roman J., Filho M., Sánchez Almeida J., 2017, ApJ, 836, 191
van der Burg R. F. J., Muzzin A., Hoekstra H., 2016, A&A, 590, A20
van Dokkum P. G., Abraham R., Merritt A., Zhang J., Geha M., Conroy C., 2015, ApJ, 798, L45
Yagi M., Koda J., Komiyama Y., Yamanoi H., 2016, ApJS, 225, 11

This paper has been typeset from a TEX/LATEX file prepared by the author.